PHYSICAL REVIEW C **95**, 061303(R) (2017)

# Search for shape-coexisting $0^+$ states in $^{66}$Ni from lifetime measurements

B. Olaizola,[1,*] L. M. Fraile,[1] H. Mach,[1,2] A. Poves,[3] F. Nowacki,[4] A. Aprahamian,[5] J. A. Briz,[6,†] J. Cal-González,[1,‡] D. Ghiţa,[7] U. Köster,[8] W. Kurcewicz,[9] S. R. Lesher,[5,10] D. Pauwels,[11] E. Picado,[1,12] D. Radulov,[11] G. S. Simpson,[13] and J. M. Udías[1]

[1]*Grupo de Física Nuclear, Facultad de Físicas, Universidad Complutense, CEI Moncloa, E-28040 Madrid, Spain*

[2]*National Centre for Nuclear Research, BP1, ul.Hoza 69, PL-00-681 Warsaw, Poland*

[3]*Departamento de Física Teórica, Universidad Autónoma, Cantoblanco, 28049, Madrid, Spain*

[4]*Institut Pluridisciplinaire Hubert Curien, CNRS et Université Louis Pasteur, F-67037 Strasbourg, France*

[5]*Department of Physics, University of Notre Dame, Notre Dame, Indiana 46556, USA*

[6]*Instituto de Estructura de la Materia, CSIC, E-28006 Madrid, Spain*

[7]*Horia Hulubei National Institute for Physics and Nuclear Engineering, P.O. Box MG-6, 077125 Bucharest-Magurele, Romania*

[8]*Institut Laue-Langevin, Boîte Postale 156, F-38042 Grenoble Cedex 9, France*

[9]*Faculty of Physics, University of Warsaw, Pasteura 5, PL 02-093 Warsaw, Poland*

[10]*Department of Physics, University of Wisconsin–La Crosse, La Crosse, Wisconsin 54601, USA*

[11]*K.U. Leuven, IKS, Celestijnenlaan 200 D, 3001 Leuven, Belgium*

[12]*Sección de Radiaciones, Departamento de Física, Universidad Nacional, Heredia, Costa Rica*

[13]*LPSC, Université Grenoble Alpes, CNRS/IN2P3, Institut National Polytechnique de Grenoble, F-38026 Grenoble Cedex, France*

(Received 20 April 2017; published 7 June 2017)

The lifetime of the $0_3^+$ state in $^{66}$Ni, two neutrons below the $N = 40$ subshell gap, has been measured. The transition $B(E2; 0_3^+ \rightarrow 2_1^+)$ is one of the most hindered $E2$ transitions in the Ni isotopic chain and it implies that, unlike $^{68}$Ni, there is a spherical structure at low excitation energy. We have performed extensive shell-model calculations that correctly predict this result, obtaining a spherical $0^+$ state at the correct energy and with an extremely low $B(E2;0_3^+ \rightarrow 2_1^+)$ value.

DOI: 10.1103/PhysRevC.95.061303

Shape coexistence in atomic nuclei occurs when low-lying states with similar energies show different intrinsic deformations. This leads to competing minima close in excitation energy. In even-even nuclei, this phenomenon is revealed by low-lying $0^+$ states, the classic example being $^{186}$Pb, where a triplet of $0^+$ states was found, associated with spherical, oblate, and prolate deformation, respectively [1]. The coexistence of nuclear shapes is closely linked to the shell gaps and how particle-hole excitations take place around them, eventually leading to deformation. Examples are abundant in regions of the nuclear chart in the proximity of shell closures and subshell closures [2].

The area around $^{68}$Ni is specially interesting, since the $N = 40$ subshell closure and the $Z = 28$ spherical magic number cohabit. The $N = 40$ subshell corresponds to a harmonic oscillator potential closure, and separates the $pf$ negative-parity shell from the spin-orbit positive-parity $g_{9/2}$ orbital. Therefore, the presence of intruder states leading to isomers and shape coexistence may be expected. In the case of $^{68}$Ni itself, $0_2^+$ is actually the first excited state, located at 1603.6 keV above the $0^+$ ground state [3]. This $0_2^+$ state has a known long half-life of 270(5) ns [4]. A third $0^+$ state is located at 2511 keV, above the 2033.0-keV $2_1^+$ state. See Fig. 1 for a systematics of all the $0^+$ states below 3 MeV in the Ni isotopic chain.

Large-scale shell-model calculations using the Lenzi-Nowacki-Poves-Sieja (LNPS) interaction [3,5–7] accurately describe the $^{68}$Ni experimental results, presenting a clear case of triple shape coexistence. The ground state is mainly comprised (60%) of a spherical configuration, corresponding to doubly magic closures at $N = 40$ and $Z = 28$. The calculations predicted an oblate-deformed $0_2^+$ as the first excited state dominated by 2p2h neutron excitations to the intruder $g_{9/2}$ orbital, with the $2_1^+$ state representing the first state of a band on top of it. The calculations also showed a prolate band built on the $0_3^+$ state and characterized by $2p2h$ proton excitations across $Z = 28$ and 4p4h–6p6h neutrons across the $N = 40$ subshell. The highly deformed band continues with the $2_2^+$ state and $B(E2; 2_2^+ \rightarrow 0_3^+) = 46$ W.u. or $\beta \sim 0.45$.

Tsunoda and collaborators [8] performed Monte Carlo shell model (MCSM) calculations for $^{68-78}$Ni, producing predictions in good agreement with the LNPS results. From the potential energy surfaces and the basis vectors in the MCSM calculations, they conclude that the $^{68}$Ni ground state is spherical, the $0_2^+$ state is oblate with a moderate deformation of the order of $\beta_2 \sim 0.2$, while the $0_3^+$ state is of prolate character, with strong deformation of $\beta_2 \sim 0.4$ corresponding to an intrinsic quadrupole moment $Q_0$ of 200 fm$^2$. In the same manner, the $2_1^+$ level at 2033 keV is identified as member of the oblate band built on the 1604 keV $0_2^+$ state, while the $2_2^+$ state at 2743 keV, above the $0_3^+$ level at 2511 keV, is consistent with a prolate nature. Nevertheless, the most recent experimental results [9] seem in better agreement with the LNPS calculations.

*bruno.olaizola@ucm.es; present address: TRIUMF, 4004 Wesbrook Mall, Vancouver, British Columbia V6T 2A3, Canada.

†Present address: CERN, Geneva 23, CH-1211 Switzerland.

‡Present address: Medical University of Vienna, Center for Medical Physics and Biomedical Engineering, Vienna, Austria.

 ©2017 American Physical Society

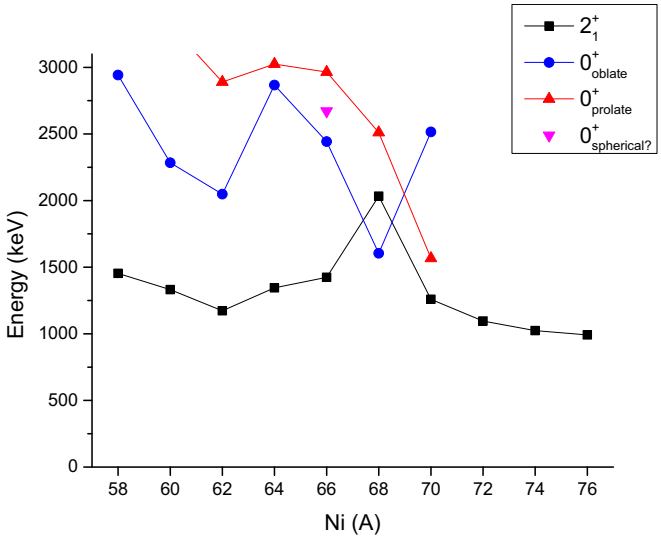


FIG. 1. Energy of the $0^+$ states below 3 MeV in the even Ni isotopes. The $2^+_1$ states have been included for reference.

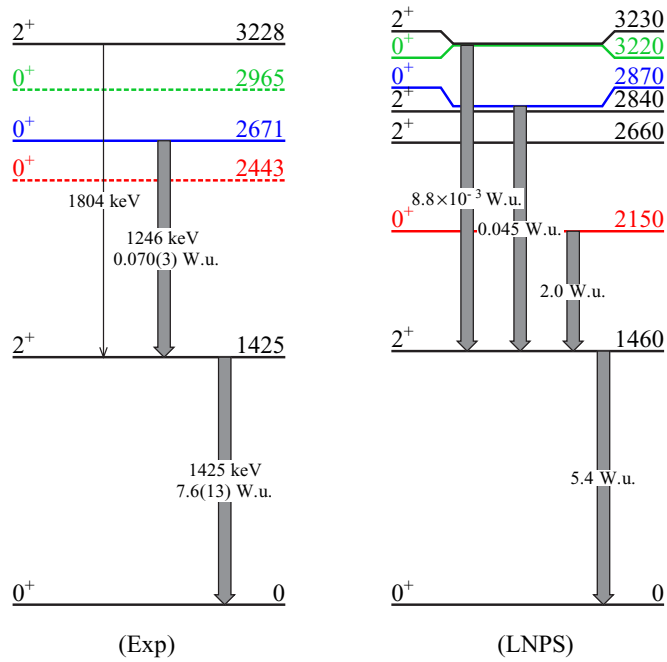


FIG. 2. (Left) $^{66}$Ni level scheme populated in the $\beta$ decay of the $(1^+)$ $^{66}$Co ground state. The dashed levels were not observed in this $\beta$-decay experiment, but have been included to help the discussion. The labels on the transitions are the energy in keV and the $B(E2)$ in W.u., while the width is proportional to their absolute intensity. (Right) Results from the LNPS calculations from this work.

Thanks to the great effort put into studying this particular nucleus over recent decades, shape coexistence in $^{68}$Ni is well established both from an experimental [3,9–12] and a theoretical point of view [3,5,8]. But the situation is not that clear for nuclei around it. Shape coexistence has been proposed for the more exotic $^{70}$Ni ($N = 42$) at even lower energy [9,13,14], and also for $^{67}$Co and $^{71}$Cu (see Refs. [15,16] and references therein), but surprisingly not for the nuclei closer to stability.

In this work, we address shape coexistence in the next even neighbor to $^{68}$Ni, the isotope $^{66}$Ni with $N = 38$. The excited structure of this nucleus is known from $\beta$ decay [10] and deep-inelastic [17] experiments. The $2^+_1$ state is located at 1425 keV, with the second $0^+_2$ state at 2443 keV and the $0^+_3$ level immediately above it at 2671 keV (see Fig. 2 for the measured $^{66}$Ni level scheme and calculations from this work). Recently Walters *et al.* [16] reported a transition connecting a new $2^+$ state to the $0^+_3$ bandhead, and proposed the levels at 2671 and 3312 keV as prolate intruder states.

The $\beta$ decay of $^{66}$Fe to $^{66}$Co was studied by D. Pauwels *et al.* [18], and they identified the $^{66}$Co ground state as a proton intruder, with a newly assigned parity of $(1^+)$ based on the strong $\beta$ feeding from the $^{66}$Fe $0^+$ ground state. The decay of $^{66}$Co only populates the ground and $0^+_3$ states and the first two $2^+$ states in $^{66}$Ni. This result was later confirmed by Liddick *et al.* [19]. A $\beta$-decay scheme of $^{66}$Co to $^{66}$Ni is shown in Fig. 2.

We have investigated experimentally the $\beta^-$ decay of $^{66}$Co to $^{66}$Ni with the aim of measuring the half-life of the excited states populated in $^{66}$Ni by means of the advanced time-delayed $\beta\gamma\gamma$(t) method described in Refs. [20–22]. This experiment was part of a wider campaign to study the evolution of collectivity below $^{68}$Ni [23–25].

The experiment was carried out at the ISOLDE facility at CERN [26]. $^{66}$Ni isotopes were populated in the $\beta$ decay chain of $A = 66$ isobars, starting from $^{66}$Mn, and 1.4-GeV protons from the CERN Proton Synchrotron Booster incident on a $UC_x$ target induced high-energy fission. Produced radionuclides were thermally released from the target and manganese atoms were ionized by the ISOLDE Resonance Ionization Laser Ion Source. Mass $A = 66$ ions were mass separated and implanted on a thin aluminium foil in the center of the experimental setup. A fast plastic scintillator acted as $\beta$ particle detector, and was placed just after the deposition point. Two truncated-cone shaped $LaBr_3$(Ce) crystals coupled to Photonis XP20D0 photomultipliers were used for $\gamma$-ray fast timing. The setup was completed by two HPGe detectors. Analog time-delayed $\beta\gamma(t)$ coincidences between the $\beta$ and each one of the $\gamma$ detectors were set up using time-to-amplitude conversion modules. The fast timing analysis is based on $\beta\gamma(t)$ distributions between the $\beta$ and $LaBr_3$(Ce) detectors and $\beta\gamma\gamma(t)$ distributions including the former and an extra condition on HPGe energies. Further details on the experimental station and data acquisition strategy can be found in Refs. [23,24].

There was no removal of the decay products and thus a saturated source including the whole $A = 66$ chain was created. Lines from the $^{66}$Co $\rightarrow$ $^{66}$Ni decay were relatively enhanced by selecting the data between 300 and 1200 ms after proton impact, when most of the $^{66}$Mn has already decayed away. A singles HPGe energy spectrum with this time condition is shown in Fig. 3. The identification of $\gamma$ rays in $^{66}$Ni is based on the existing information [10]. Despite having $\sim$50 times more statistics than the previous $\beta$-decay experiment [10], only one new transition of 2231.9 keV has been observed. This transition is in clear coincidence with the 1425-keV $\gamma$ ray,

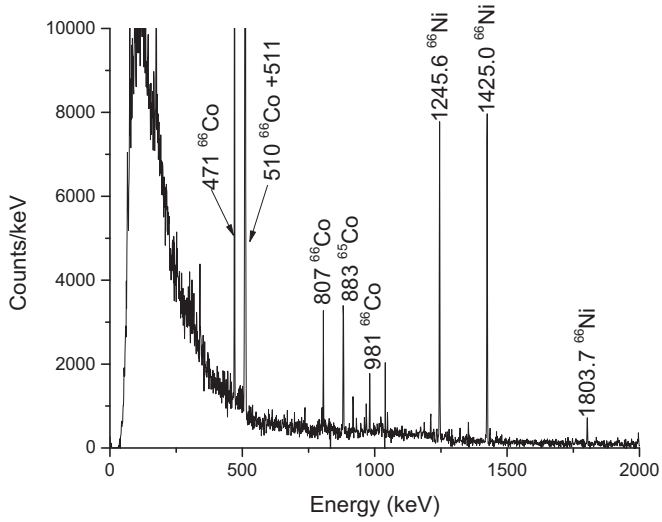


FIG. 3. Singles HPGe energy spectrum. A time gate of 300–1200 ms after the proton impact on the target was selected to enhance the $^{66}$Co decay activity. The long-lived $^{66}$Ga contaminant was subtracted. This did not suppress the $^{66}$Fe decay activity, so the transitions in $^{66}$Co are present and labeled in the spectrum.

but it is not observed in the singles spectrum, so its placement in the level scheme is uncertain. On a side note, we can confirm the unambiguous assignment of the 471-keV transition to the decay of $^{66}$Fe to $^{66}$Co, as was already proposed in Ref. [19], and in contrast to the suggestion made in Ref. [27]. We also found no trace of the 1020(1)-keV transition proposed in Ref. [27] nor the 1018- and 1478-keV lines suggested in Ref. [17]. These lines should be in coincidence with the 1425-keV transition to the ground state and, in spite of our sufficient amount of statistics, they were not found; see Fig. 4.

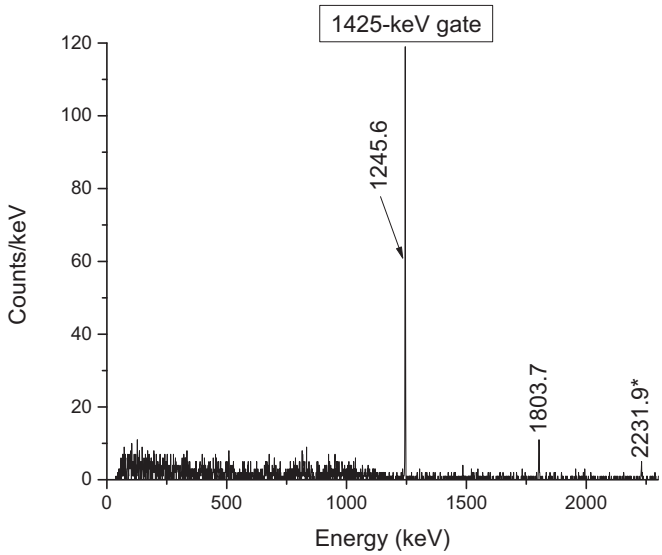


FIG. 4. Coincidence HPGe-HPGe energy spectrum with a gate on the 1425-keV transition. An asterisk (*) denotes a new transition of 2231.9 keV observed for the first time; see text for details.

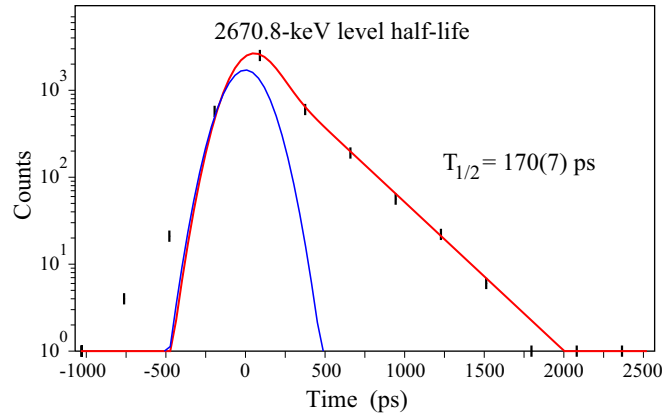


FIG. 5. Fit to the 2671-keV level half-life in $^{66}$Ni using the time difference between a $\beta$ and the 1246-keV decay transition detected in one of the $LaBr_3$(Ce) crystals. The fit was done to a prompt Gaussian including the Compton background under the peak and a decay exponential. The result of $T_{1/2} = 170(7)$ ps stems from the weighted average of four measurements. See text for details.

The $^{66}$Co $\beta^-$ decay mainly populates the ground state and the $0_3^+$ level at 2671 keV with $I_\beta = 29(3)\%$ [18]. The $0_2^+$ level at 2443 keV and the $0_4^+$ at 2965(10) keV are not populated in the decay of the $^{66}$Co $(1^+)$ ground state, pointing towards a substantially different nuclear structure. The $0_3^+$ state de-excites to the $2_1^+$ level at 1425 keV via a $\gamma$-ray of 1246 keV [10,27], and the $2_1^+$ feeds the ground state with a 1425-keV transition.

Figure 5 shows the $\beta - LaBr_3$(Ce) time difference with an energy gate in the 1246-keV $0_3^+ \rightarrow 2_1^+$ transition. This slope is identical to the one obtained with a condition on the 1425-keV $2_1^+ \rightarrow 0_1^+$ peak and is not present if the gate is selected in the Compton background above each of the full-energy peaks. The half-life is therefore assigned to the $0_3^+$ 2671-keV level unambiguously. The observed slope in the 1425-keV gate is consistent with feeding via the 1246-keV $\gamma$ ray, since the direct $\beta$ feeding to the $2_1^+$ 1425-keV state is about 6 times lower than the $\beta$ feeding to the 2671-keV state. In this manner, the half-life is measured independently using two different $\gamma$ transitions selected in the $LaBr_3$(Ce) detectors and using two different crystals. The four lifetime measurements are consistent and yield a weighted average value of $T_{1/2} = 170(7)$ ps. The calculated $B(E2; 0_3^+ \rightarrow 2_1^+)$ value is 1.11(5) $e^2$ fm$^4$ or 0.070(3) W.u.

Since no transitions are observed feeding the $0_3^+$ state from above (Fig. 6 shows only the $2_1^+ \rightarrow 0_1^+$ transition in coincidence), we can discard any significant contribution to the half-life from higher energy levels.

This result was further cross-checked in $\beta\gamma\gamma$(t) coincidences. Either by selecting the 1246-keV transition in the $LaBr_3$(Ce) and the 1425-keV in the HPGe detector or vice versa, a slope compatible with a half-life of a few hundreds of picoseconds was observed in the delayed part. However, in this restrictive coincidence conditions the statistics were much lower and the resulting half-life, even if compatible with the $\beta\gamma$ result, had a much larger error bar.

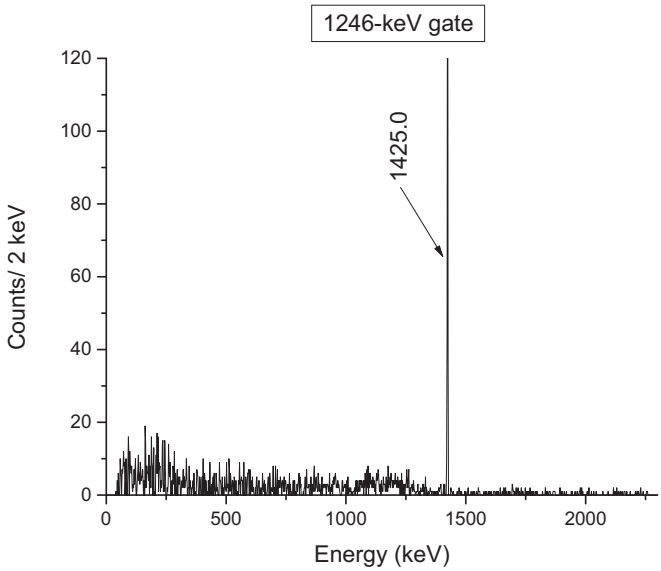


FIG. 6. Coincidence HPGe-HPGe energy spectrum with a gate on the 1246-keV transition, showing the 1425-keV line.

The measured value can be compared to a similar state in $^{68}$Ni, where a recent study by Crider *et al.* [9] reports a $T_{1/2} = 570(50)$ ps for the 2511-keV state via the 478-keV de-exciting transition. In terms of transition probabilities, Crider *et al.* [9] obtained a $B(E2; 0_3^+ \rightarrow 2_1^+)$ of 39.0(34) e$^2$ fm$^4$ using a 98.1% lower limit for the branching ratio. With this result, they proposed the $0_3^+$ state to be of prolate nature. From the lifetime in $^{66}$Ni measured in this work, and neglecting any $E0$ decay branches to the ground and $0_2^+$ states, the $B(E2)$ obtained is 1.11(5) e$^2$ fm$^4$, around 35 times slower. Any $E0$ branch in $^{66}$Ni would make the $B(E2; 0_3^+ \rightarrow 2_1^+)$ value even lower.

This result clearly implies that the $0_3^+$ states in $^{66}$Ni and $^{68}$Ni are not of the same nature, eliminating the possibility that the $0_3^+$ is the prolate state in $^{66}$Ni contrary to the proposal in Ref. [16]. One final argument that can be made is the different population of the $0^+$ states by the $^{66}$Co $\beta$ decay. It strongly populates the $0_1^+$ and $0_3^+$, while no population has been observed for the $0_2^+$ and $0_4^+$. If the ground state of $^{66}$Co is a deformed proton intruder state from the $pf$ orbitals as argued in Refs. [18,19], the selection rule requires that $\beta$ decay populates states in $^{66}$Ni by allowed transitions; therefore, neutrons in the $pf$ orbitals, as opposed to population of neutrons in the $g_{9/2}$ orbital, which would require a first forbidden transition. In this region, states based on neutrons in the $pf$ orbital are of spherical nature, contrary to the $g_{9/2}$ orbital, which carries deformation.

To gain insight in the nuclear structure of $^{66}$Ni, we performed extensive shell-model calculations using the LNPS interaction [5]. The configuration space was extended up to 14p-14h excitations across the $Z = 28$ and $N = 40$ shell gaps to achieve energy convergence. The corresponding basis dimension amounts to $2 \times 10^9$ Slater determinants basis. Effective charges of 1.31 for the protons and 0.46 for the neutrons were adopted from the microscopic calculation of

TABLE I. Summary of the key results of the LNPS calculations performed for $^{66}$Ni. Columns 4 to 6 give the particle occupation of the orbitals. $\beta_s$ and $\gamma_s$ are the deformation and the deviation from axial symmetry as defined by Kumar [29]. $Q_s$ is the intrinsic quadrupole moment of the sum-rule $2^+$ state built upon each $0^+$ state.

| Level | Exp. $E$ (MeV) | Calc. $E$ (MeV) | $\pi f_{7/2}$ | $\nu g_{9/2}$ | $\nu d_{5/2}$ | $\beta_s$ | $\gamma_s$ | $Q_s$ (e fm$^2$) |
|---|---|---|---|---|---|---|---|---|
| $0_1^+$ | 0 | 0 | 6.6 | 1.0 | 0.1 | 0.20 | 39° | 12.4 |
| $0_2^+$ | 2.443 | 2.15 | 6.0 | 2.0 | 0.2 | 0.25 | 36° | 11.2 |
| $0_3^+$ | 2.671 | 2.87 | 6.7 | 0.5 | 0.1 | 0.17 | 36° | 6.4 |
| $0_4^+$ | 2.965 | 3.22 | 5.1 | 3.1 | 0.7 | 0.39 | 12° | −44.7 |

Ref. [28]. Our results, summarized in Table I, clearly show that the $0_3^+$ state is dominated by the spherical two neutron-hole configuration in the $pf$ orbitals. This $0_3^+$ state has the lowest deformation of the $0^+$ levels in $^{66}$Ni, and can be compared to the spherical ground state in $^{68}$Ni.

The shell-model calculations showed in Table I also hint that $^{66}$Ni is not a clearcut case of shape coexistence. The $0_2^+$ presents a weakly deformed oblate structure, based on a two-neutron excitation from the $pf$ to the $g_{9/2}$ orbital, and can be considered to have a similar structure than the $0_2^+$ level in $^{68}$Ni. The $0_4^+$ state shows a high prolate deformation of $\beta = 0.39$. Only in this state is the $d_{5/2}$ occupation not negligible. This state can be matched to the $0_3^+$ state in $^{68}$Ni. Finally, the $^{66}$Ni ground state would be an admixture of the $0_2^+$ and $0_3^+$ states, with a slight oblate deformation.

These results are consistent with the $^{64}$Ni$(t,p)^{66}$Ni experiment described in Ref. [30], where an enhanced relative yield of the $0_1^+$ and $0_3^+$ states in the reaction are reported, while the $0_4^+$ population is suppressed, pointing to a possible deformed configuration for the latter level, compared to a spherical one of the other two.

As a stringent test of the shell-model calculations, the calculated $B(E2)$ values were compared to the experimental results; see Fig. 2. It is worth noting the excellent agreement between the calculated energies and the experimental ones, as well as the $B(E2; 2_1^+ \rightarrow 0_1^+)$ and $B(E2; 0_3^+ \rightarrow 2_1^+)$ values.

Our result can be compared with neighboring isotopes. Table II shows all the experimental values of the $B(E2; 0_i^+ \rightarrow 2_1^+)$ transitions measured in the Ni isotopic chain. The result presented in this paper is more than one order of magnitude smaller than that of similar transitions in the region. This slow transition clearly points out that $^{66}$Ni is comprised of different nuclear structures than the rest of the isotopic chain. If we compare the $B(E2; 0_2^+ \rightarrow 2_1^+)$ (the $E2$ transition from the prolate $0^+$ state to the first $2^+$) in $^{70}$Ni (two neutrons above $^{68}$Ni), we can see that it is at least 50 times faster than the $B(E2; 0_3^+ \rightarrow 2_1^+)$ in $^{66}$Ni (two neutrons below $^{68}$Ni). We can safely discard this $0_3^+$ in $^{66}$Ni as the same prolate state as in $^{70}$Ni.

We need to go to $^{58}$Ni to find a transition with such retardation as the one observed here. The $0_2^+$ presents one of the smallest $\rho^2$ ($E0$) observed [36]. But this level also has the lowest $B(E2)$ of the Ni isotopes, with $B(E2; 0_2^+ \rightarrow 2_1^+) = 4.0(6) \times 10^{-4}$ W.u. (moreover, it is one of the most hindered

TABLE II. Summary of the known B(E2;$0_i^+ \rightarrow 2_1^+$) in the Ni isotopic chain.

| Isotope | Transition | $B(E2)$ (W.u.) | Reference |
|---|---|---|---|
| $^{58}$Ni | $0_2^+ \rightarrow 2_1^+$ | $4.0(6) \times 10^{-4}$ | [31] |
| | $0_3^+ \rightarrow 2_1^+$ | 5.6(18) | [32] |
| $^{60}$Ni | $0_2^+ \rightarrow 2_1^+$ | <71 | [33] |
| | $0_3^+ \rightarrow 2_1^+$ | 9(3) | [33] |
| $^{62}$Ni | $0_2^+ \rightarrow 2_1^+$ | 42(22) | [34] |
| | $0_3^+ \rightarrow 2_1^+$ | <0.84 | [35] |
| $^{64}$Ni | $0_2^+ \rightarrow 2_1^+$ | 110(60) | [33] |
| $^{66}$Ni | $0_3^+ \rightarrow 2_1^+$ | 0.070(3) | This work |
| $^{68}$Ni | $0_3^+ \rightarrow 2_1^+$ | 2.4(2) | [9] |
| $^{70}$Ni | $0_2^+ \rightarrow 2_1^+$ | >3.4 | [9] |

transitions ever observed). There is some parallelism between the two isotopes, as $^{58}$Ni can be explained as a core with two extra neutrons in the $p_{3/2}f_{5/2}p_{1/2}$ orbitals while $^{66}$Ni would be also a core with two neutron holes in the same orbitals.

Möller *et al.* [37] calculated the existence of nuclear shape isomers for a vast range of nuclei and predicted a spherical ground state for $^{66}$Ni with a prolate $0^+$ at 2.67 MeV. Despite the excellent agreement with the experimental energy and the long lifetime of the $0_3^+$ state, our results clearly indicate that this state is spherical. Thus the data and calculations presented in this work clearly discard the third $0^+$ as the predicted shape isomer, leaving the second and fourth $0^+$ states as candidates.

In conclusion, we present direct evidence through the measurement of the $0_3^+$ state lifetime and by large-scale shell-model calculations, of the presence of a spherical structure at low energies in $^{66}$Ni. Moreover, these calculations also suggest that, unlike the neighboring $^{68}$Ni, $^{66}$Ni is not a clear case of shape coexistence, with a significant mixing of the different bands at low energy. The measured $B(E2; 0_3^+ \rightarrow 2_1^+)$ is exceptionally low and is the second lowest $B(E2)$ transition rate in the Ni isotopic chain.

*Note added.* During the review process, we have been made aware of a very recent publication [38] reporting an independent measurement of the same quantity by a complementary method and including lifetime measurements of the other $0^+$ states. Their measured lifetime for the $0_3^+$ is more than $2\sigma$ away from our value. While statistically speaking these two values are not in agreement, the underlying physics interpretation of the state and the nucleus is the same in both cases. The Monte Carlo shell model calculations in Ref. [38] are in remarkable accordance with the calculations presented in this work.

## ACKNOWLEDGMENTS

This work was partially supported by the Spanish MINECO through projects FPA2013-41267-P, FPA2014-57196, FPA2015-65035-P, and the NuPNET network FATIMA (PRI-PIMNUP-2011-1338). The support by the European Union Seventh Framework through ENSAR (Contract No. 262010) is acknowledged. Fast timing electronics were provided by the Fast Timing Collaboration and MASTICON. B.O. acknowledges funding by the CPAN project (CSD-2007-00042@ Ingenio 2010). A.A. and S.R.L. acknowledge funding by the US National Science Foundation under Contract No. PHY-07-58100. J.A.B. acknowledges funding by the Spanish MINECO through Project FPA2012-32443. A.P. is partly funded by Programme "Centros de Excelencia Severo Ochoa" (SEV-2012-0249).

[1] P. Van Duppen and M. Huyse, Hyperfine Interact. **129**, 149 (2000).
[2] K. Heyde and J. L. Wood, Rev. Mod. Phys. **83**, 1467 (2011).
[3] F. Flavigny, D. Pauwels, D. Radulov, I. J. Darby, H. De Witte, J. Diriken, D. V. Fedorov, V. N. Fedosseev, L. M. Fraile, M. Huyse *et al.*, Phys. Rev. C **91**, 034310 (2015).
[4] O. Sorlin, S. Leenhardt, C. Donzaud, J. Duprat, F. Azaiez, F. Nowacki, H. Grawe, Z. Dombrádi, F. Amorini, A. Astier *et al.*, Phys. Rev. Lett. **88**, 092501 (2002).
[5] S. M. Lenzi, F. Nowacki, A. Poves, and K. Sieja, Phys. Rev. C **82**, 054301 (2010).
[6] A. Dijon, E. Clément, G. de France, G. de Angelis, G. Duchêne, J. Dudouet, S. Franchoo, A. Gadea, A. Gottardo, T. Hüyük *et al.*, Phys. Rev. C **85**, 031301 (2012).
[7] A. Poves, J. Phys. G: Nucl. Part. Phys. **43**, 024010 (2016).
[8] Y. Tsunoda, T. Otsuka, N. Shimizu, M. Honma, and Y. Utsuno, Phys. Rev. C **89**, 031301 (2014).
[9] B. Crider, C. Prokop, S. Liddick, M. Al-Shudifat, A. Ayangeakaa, M. Carpenter, J. Carroll, J. Chen, C. Chiara, H. David *et al.*, Phys. Lett. B **763**, 108 (2016).
[10] W. F. Mueller, B. Bruyneel, S. Franchoo, M. Huyse, J. Kurpeta, K. Kruglov, Y. Kudryavtsev, N. V. S. V. Prasad, R. Raabe, I. Reusen *et al.*, Phys. Rev. C **61**, 054308 (2000).
[11] F. Recchia, C. J. Chiara, R. V. F. Janssens, D. Weisshaar, A. Gade, W. B. Walters, M. Albers, M. Alcorta, V. M. Bader, T. Baugher *et al.*, Phys. Rev. C **88**, 041302 (2013).
[12] S. Suchyta, S. N. Liddick, Y. Tsunoda, T. Otsuka, M. B. Bennett, A. Chemey, M. Honma, N. Larson, C. J. Prokop, S. J. Quinn *et al.*, Phys. Rev. C **89**, 021301 (2014).
[13] C. J. Chiara, D. Weisshaar, R. V. F. Janssens, Y. Tsunoda, T. Otsuka, J. L. Harker, W. B. Walters, F. Recchia, M. Albers, M. Alcorta *et al.*, Phys. Rev. C **91**, 044309 (2015).
[14] C. J. Prokop, B. P. Crider, S. N. Liddick, A. D. Ayangeakaa, M. P. Carpenter, J. J. Carroll, J. Chen, C. J. Chiara, H. M. David, A. C. Dombos *et al.*, Phys. Rev. C **92**, 061302 (2015).
[15] D. Pauwels, O. Ivanov, N. Bree, J. Büscher, T. E. Cocolios, J. Gentens, M. Huyse, A. Korgul, Y. Kudryavtsev, R. Raabe *et al.*, Phys. Rev. C **78**, 041307 (2008).
[16] W. B. Walters, C. J. Chiara, R. V. F. Janssens, D. Weisshaar, T. Otsuka, Y. Tsunoda, F. Recchia, A. Gade, J. L. Harker, M. Albers *et al.*, AIP Conf. Proc. **1681**, 030007 (2015).
[17] R. Broda, T. Pawłat, W. Królas, R. V. F. Janssens, S. Zhu, W. B. Walters, B. Fornal, C. J. Chiara, M. P. Carpenter, N. Hoteling *et al.*, Phys. Rev. C **86**, 064312 (2012).

[18] D. Pauwels, D. Radulov, I. Darby, H. De Witte, J. Diriken, D. Fedorov, V. Fedosseev, L. Fraile, M. Huyse, U. Köster *et al.*, ARIS2011 Conference (2011), https://iks32.fys.kuleuven.be/indico/event/0/session/17/contribution/158.
[19] S. N. Liddick, B. Abromeit, A. Ayres, A. Bey, C. R. Bingham, M. Bolla, L. Cartegni, H. L. Crawford, I. G. Darby, R. Grzywacz *et al.*, Phys. Rev. C **85**, 014328 (2012).
[20] H. Mach, R. Gill, and M. Moszyński, Nucl. Instr. Methods Phys. Res. A **280**, 49 (1989).
[21] M. Moszyński and H. Mach, Nucl. Instr. Methods Phys. Res. A **277**, 407 (1989).
[22] H. Mach, F. Wohn, G. Molnár, K. Sistemich, J. C. Hill, M. Moszyński, R. Gill, W. Krips, and D. Brenner, Nucl. Phys. A **523**, 197 (1991).
[23] B. Olaizola, L. M. Fraile, H. Mach, A. Aprahamian, J. A. Briz, J. Cal-González, D. Ghia, U. Klez, D. Ghia, U. Köster, W. Kurcewicz, S. R. Lesher, D. Pauwels, E. Picado, A. Poves, D. Radulov, G. S. Simpson, and J. M. Udías, Phys. Rev. C **88**, 044306 (2013).
[24] B. Olaizola, Ultra-fast timing study of exotic neutron-rich isotopes, Ph.D. thesis, Universidad Complutense de Madrid, Spain, 2013.
[25] B. Olaizola, L. M. Fraile, H. Mach, A. Aprahamian, J. A. Briz, J. Cal-González, D. Ghiţa, U. Köster, W. Kurcewicz, S. R. Lesher *et al.*, JPS Conf. Proc **6**, 030006 (2015).
[26] E. Kugler, Hyperfine Interact. **129**, 23 (2000).
[27] U. Bosch, W.-D. Schmidt-Ott, E. Runte, P. Tidemand-Petersson, P. Koschel, F. Meissner, R. Kirchner, O. Klepper, E. Roeckl, K. Rykaczewski, and D. Schardt, Nucl. Phys. A **477**, 89 (1988).
[28] M. Dufour and A. P. Zuker, Phys. Rev. C **54**, 1641 (1996).
[29] K. Kumar, Phys. Rev. Lett. **28**, 249 (1972).
[30] W. Darcey, R. Chapman, and S. Hinds, Nucl. Phys. A **170**, 253 (1971).
[31] S. Raman, Nucl. Phys. A **158**, 65 (1970).
[32] M. C. Bertin, N. Benczer-Koller, G. G. Seaman, and J. R. MacDonald, Phys. Rev. **183**, 964 (1969).
[33] Y. G. Kosyak, D. K. Kaipov, and L. V. Chekushina, Izv. Akad. Nauk SSSR, Ser. Fiz. **53**, 2130 (1989) [Bull. Acad. Sci. USSR, Phys. Ser. **53**(11), 68 (1989)].
[34] A. Chakraborty, J. N. Orce, S. F. Ashley, B. A. Brown, B. P. Crider, E. Elhami, M. T. McEllistrem, S. Mukhopadhyay, E. E. Peters, B. Singh, and S. W. Yates, Phys. Rev. C **83**, 034316 (2011).
[35] D. Kennedy, H. Bolotin, I. Morrison, and K. Amos, Nucl. Phys. A **308**, 14 (1978).
[36] T. Kibédi and R. Spear, At. Data Nucl. Data Tables **89**, 77 (2005).
[37] P. Möller, A. Sierk, R. Bengtsson, H. Sagawa, and T. Ichikawa, At. Data Nucl. Data Tables **98**, 149 (2012).
[38] S. Leoni, B. Fornal, N. Mărginean, M. Sferrazza, Y. Tsunoda, T. Otsuka, G. Bocchi, F. C. L. Crespi, A. Bracco, S. Aydin *et al.*, Phys. Rev. Lett. **118**, 162502 (2017).